INTERNATIONAL JOURNAL OF CLIMATOLOGY
Int. J. Climatol. **27**: 189–209 (2007)
Published online 6 December 2006 in Wiley InterScience
(www.interscience.wiley.com) DOI: 10.1002/joc.1385

RMetS
ROYAL METEOROLOGICAL SOCIETY

The tropopause at southern extratropical latitudes: Argentine operational rawinsonde climatology

Susana A. Bischoff,[a]* Pablo O. Canziani[a,b] and Adrián E. Yuchechen[b]

[a] *Departamento de Ciencias de la Atmósfera y los Océanos – Facultad de Ciencias Exactas y Naturales, Universidad de Buenos Aires, Argentina*
[b] *Programa de Estudio de Procesos Atmosféricos en el Cambio Global (PEPACG), Pontificia Universidad Católica Argentina (UCA)/Consejo Nacional de Investigaciones Científicas y Técnicas (CONICET)*

Abstract:

Argentine operational rawinsonde records spanning a 30-year period (1968–1997) were used to study the climatology of the tropopause from the subtropics to the southern mid-latitudes, approximately along the 60 °W meridian. The thermal tropopause annual cycle as well as its variability was analyzed at three sites: Resistencia (RES), Ezeiza (EZE), and Comodoro Rivadavia (CRD). Single and double tropopause observations were studied, given the comparatively frequent occurrence of double tropopause events at all three sites. The tropopause behavior at RES and CRD is distinct, whereas at EZE it shows a winter evolution similar to the one at CRD and a summer evolution closer to the one at RES, in agreement with the annual evolution of the subtropical jet. The tropopause evolution is discussed under the light of the dynamic climatology of southern South America. In the presence of double tropopause events and in terms of potential temperature, it should be noted that the upper tropopause temperature is close to the 380 K isentropic, i.e. the tropical tropopause layer. Moreover, the lower tropopause and single tropopause events are fairly close together, i.e. coincident with the lowermost stratosphere. Considering previous research and results from the present analysis, a definition of Extratropical Tropopause Layer (ExTL) is introduced in this work. It is proposed that the lowermost stratosphere should be regarded as the ExTL. Copyright © 2006 Royal Meteorological Society

KEY WORDS tropopause climatology; single tropopause; double tropopause; stratosphere; troposphere

Received 18 November 2005; Revised 7 June 2006; Accepted 10 June 2006

INTRODUCTION

Various studies carried out during the last decade have shown that a more detailed understanding of the tropopause is required. This narrow atmospheric region has appeared as a crucial component of the troposphere–stratosphere system, playing a part in the evolution of the ozone layer (Hoerling *et al*., 1991; Steinbrecht *et al*., 1998), as well as in the climate and climate change processes (Brasseur, 1997; Gaffen *et al*., 2000) and the exchange of various species such as CFCs and greenhouse gases (Shapiro, 1980; Wirth, 1995; Holton, 1990). A simple explanation for the existence of the tropopause can be found in Thuburn and Craig (1997) with the aid of an old radiative-convective model. That explanation works well in trying to depict the tropical tropopause behavior, but it cannot explain the tropopause height distribution in regions other than the tropical region.

Hoinka (1997) and Gettelman and Forster (2002) have reviewed various aspects of studies of the tropopause during the last hundred years. After the observations made by Léon Teisserenc de Bort and Richard Assman over a hundred years ago (Labitzke and Van Loon, 1999), 50 years went by until a comprehensive observation of the global tropopause could be reached. Indeed, with the global expansion of the rawinsonde operational network during the International Geophysical Year (1957–1958), a global coverage of the troposphere and lower stratosphere became possible almost on a daily basis. Microwave Sounding Unit (MSU) sensors, flying on NOAA satellites since late 1978, have provided global temperature retrievals near 100 hPa, which is often compared to (or used as) a proxy for tropopause temperatures in the tropics. A wide description of the MSU sensors can be found in Smith *et al*. (1979) and Spencer *et al*. (1990). More recently, temperature profiles derived from the Global Positioning System (GPS) provide an extensive coverage of the upper troposphere/lower stratosphere temperatures (Lakkis, 2005; Yuchechen *et al*., submitted, 2005). The use of GPS satellites to observe the Earth's atmosphere is presented in Kursinski *et al*. (1997). Hoinka (1997, 1998 and 1999) has carried out a global study of the tropopause using ECWMF reanalysis products and Nielsen-Gammon (2001) has provided visual analysis products from the NCEP reanalysis. More recently, Reichler *et al*. (2003) made a comparison

* Correspondence to: Susana A. Bischoff, Departamento de Ciencias de la Atmósfera y los Océanos, Facultad de Ciencias Exactas y Naturales, Universidad de Buenos Aires, Pabellón II, Ciudad Universitaria, 1428-Capital Federal, República Argentina. E-mail: bischoff@at.fcen.uba.ar

Copyright © 2006 Royal Meteorological Society

WILEY InterScience® DISCOVER SOMETHING GREAT

between the tropopause height calculated from gridded data and the tropopause height obtained by observations from upper air stations.

The tropopause can be defined in several ways, the most common being the World Meteorological Organization (WMO) definition: 'The boundary between the troposphere and the stratosphere, where an abrupt change in lapse rate usually occurs. It is defined as the lowest level at which the lapse rate decreases to 2 °C km^{-1} or less, provided that the average lapse rate between this level and all higher levels within 2 km does not exceed 2 °C km^{-1}' WMO (1992). This definition is referred to as the *thermal tropopause*, and is the definition used in the operational rawinsonde profile retrievals. Sometimes the *cold-point tropopause* has been used in terms of the coldest point in the temperature profile.

The tropopause can also be defined in terms of the discontinuity observed in the Ertel's Potential Vorticity (PV) (e.g. Reed, 1955; Hoerling *et al*., 1991; Hoinka, 1997; Shepherd, 2002) and is referred to as *dynamic tropopause*. However, such a definition requires the evaluation of horizontal gradients of the wind field from upper air analysis, and thus its use in data sparse areas is limited, unless regional or global analysis products are considered. Besides, Ertel's PV shows an exponential variation with height. Lait (1994) described a form of PV that has conservation properties similar to those of Ertel's PV, but removes this exponential variation with height in terms of a 'modified PV'.

There are several PV values that can be considered to define the dynamic tropopause, as discussed in Hoinka (1997). When processing rawinsonde data, there is a way to determine the dynamic tropopause (Bleck and Mattocks, 1984), but the density of rawinsondes should be sufficiently high for this method to work well. Normally, this method will not be useful in the Southern Hemisphere (SH).

In terms of the vertical distribution of ozone, it is also possible to determine a *chemical tropopause*, which undergoes a rapid increase in concentration in the vicinity of the tropopause (Hoinka, 1997). Using a global circulation model, Thuburn and Craig (1997) showed that the ozone distribution does not play a crucial role in the tropopause height distribution; nevertheless, the temperature at the earth's surface is a very important parameter in determining it.

It should be noted that the tropopause may also occur as a multiple or layered tropopause. Bjerknes and Palmén (1937), Kochanski (1955), and Godske *et al*. (1957) have already referred to their occurrence. Defant and Taba (1957, 1958) mentioned the occurrence of multiple tropopause events in their study of air masses over the Northern Hemisphere (NH). Huschke (1959) pointed out that multiple tropopause events are common 'above regions of large horizontal temperature contrast in the troposphere'. WMO (1992) also defines the occurrence of a second tropopause: 'Occasionally, a second tropopause may be found if the lapse rate above the first tropopause exceeds 3 °C km^{-1}'. Multiple tropopauses are also defined by WMO (1992): 'A frequent atmospheric condition in which the tropopause appears not as a continuous single "surface" of discontinuity between the troposphere and the stratosphere, but as a series of quasi horizontal "leaves" which are partly overlapping in a step-like arrangement'. Hence, the tropopause is now more frequently viewed as a comparatively narrow region or layer separating the troposphere from the stratosphere rather than as a thin material surface. Please note that Willett (1944) had already viewed the tropopause as a layer. Thus the tropopause (or the first tropopause in case of double or multiple tropopause events) can be viewed as the point where the transition from the troposphere into the stratosphere begins.

Many recent studies have dealt with the tropopause in the tropics, i.e. Tropical Tropopause Layer (TTL) (e.g. Gettelman and Forster, 2002; Seidel *et al*., 2001, and references therein) and to a lesser extent in Polar Regions (e.g. Zängl and Hoinka, 2001). However, mid-latitude/extratropical studies – which, by extension, we shall refer to as the Extratropical Tropopause Layer (ExTL) – have been scant. As pointed out in Shepherd (2002), the mechanisms that result in the ExTL formation are different from those that result in the TTL formation. The ExTL is of interest since there are a number of processes that are influenced by its behavior. In the first place, the changes in the total column of ozone can be referred to the changes in tropopause height (e.g. Steinbrecht *et al*., 1998; Salby and Callaghan, 1993; Canziani *et al*., 2002). It appears that some of the trends in total ozone could be due not only to depletion by chemical processes but also as a result of long-term changes in tropopause height. However, the exact relationship between long-term changes in tropopause and changes in ozone remains unclear (WMO, 2003). Such a process could well establish a link between climate variability/change and the evolution of the ozone layer at mid to high latitudes. Furthermore, the contribution to stratosphere–troposphere exchange may not be negligible at those latitudes (Appenzeller *et al*., 1996). The evolution of the ExTL may influence local and regional climate processes through its interactions with the propagating wave systems. A number of studies have shown that PV near the tropopause or changes in the tropopause location influences the synoptic systems (e.g. Morgan and Nielsen-Gammon, 1998). It should be noted that, to the best of our knowledge, there were no studies – at least during the last decade or so – making any reference to multiple tropopause events, other than those concentrating on tropopause fold events (e.g. Van Haver *et al*., 1996). Only recently Pan *et al*. (2004) did study double tropopause events over the NH.

There are virtually no recent studies referring to the SH ExTL other than Velasco and Necco (1981), and the previously referenced research by Hoinka (1998). Given the characteristics of the reanalysis products and the manner that the tropopause is derived thereof (e.g. Hoinka, 1997; Reichler *et al*., 2003), it is not possible to determine multiple tropopause events in analysis-/reanalysis-based

Copyright © 2006 Royal Meteorological Society

DOI: 10.1002/joc

studies. Seidel *et al*. (2001) discuss other aspects of the limitation in the use of the analysis-/reanalysis-derived tropopauses. Even rawinsonde data studies do not mention the occurrence of such events.

Hence, it is necessary to develop an understanding of the ExTL and its climatology. In order to fill this gap and considering that it is essential to establish a truly observational climatology, a network of three Argentine operational rawinsonde stations, spanning a narrow longitude segment and covering 30 years of observations, was selected to initiate the development of such climatology. The latitudinal extent of the network allows comparison of the tropopause behavior from the lower subtropics into the mid-latitudes. The corresponding data set was used to establish an ExTL climatology for southern South America, along the Atlantic coast. The occurrence and statistics of single and double tropopause events were specifically analyzed. The paper is organized as follows. In Section 2, the nature and the quality of the observations are discussed. Section 3 presents the results of the climatology, including a detailed analysis of the seasonal behavior and the physical processes involved. Section 4 presents a discussion of the results under the scope of seasonal and synoptic processes in the region. Concluding remarks are found in Section 5.

DATA

Three stations from the Argentine operational rawinsonde network, operated by the Argentine Servicio Meteorológico Nacional (SMN), were chosen to establish a North–South network with extended time coverage. The chosen stations are Resistencia (RES) ($\varphi = 27.45\,^{\circ}$S, $\lambda = 59.05\,^{\circ}$W), Ezeiza (EZE) ($\varphi = 34.81\,^{\circ}$S, $\lambda = 58.53\,^{\circ}$W), and Comodoro Rivadavia (CRD) ($\varphi = 45.78\,^{\circ}$S, $\lambda = 67.50\,^{\circ}$W). Stations will be referred to hereafter using the International Air Transport Association (IATA) three-character location identifier: RES, EZE, and CRD. The data sets span a 30-year period (from 1968 to 1997) and do not include tropopauses higher than 100 hPa, owing to the scant number of rawinsonde balloons surviving above that height. Note, nevertheless, that this implies that approximately 8000–9000 profiles per station were analyzed in this study.

These three stations provide insights into the different ExTL regimes, CRD being a mid-latitude site and RES being close to the tropical edge of the subtropics. As will be seen later, EZE can be viewed as an intermediate region, influenced by both the tropics and the mid-latitude systems.

The thermal tropopause was determined following the WMO definitions (WMO, 1957, 1992), both in the case of the single tropopause events (*S-events*) and double tropopause ones (*D-events*). The data set used in this study is restricted to 12 UTC. It doesn't make any difference to refer to single tropopause events as *ST* or *S-events*. However, there is ambiguity with double tropopause events. In these cases, the lower tropopause will be referred to as *double first tropopause* (*DF*), while the upper one will be referred to as *double second tropopause* (*DS*).

Before proceeding further, with respect to the information obtained from rawinsondes, it is important to note that historical data sets have undergone changes over time because of a variety of factors. These include the use of different rawinsonde models and the applications of different observation methods for retrieving the upper atmosphere temperature, which are dependent on sensor models, changes in the solar radiation corrections applied to the data, and even changes resulting from modifications to the length of the cord that ties the instrument to the balloon. Such changes can lead to discontinuities of a few tenths of a degree per decade in the temperature record, but it can also happen that discontinuities are of the order of temperature trends, as has been shown in many rawinsonde-related research efforts. For instance, Angell (1991) points out that, over a network formed by 63 stations, 43% of them have inhomogeneities, and that these inhomogeneities are more common in the stratosphere. Cox and Parker (1992) made a description of the sources for inhomogeneities present in the series. Luers and Eskridge (1998) evaluated the potential use of temperature obtained by ten of the most common rawinsondes used since 1960 for climatic studies. Other researches using rawinsonde-retrieved information are Suzuki and Asahi (1978), WMO (1978), Huovila and Tuominen (1990), Elliott and Gaffen (1991), and Duarte and Bischoff (1998), just to mention a few.

The introduction of a new rawinsonde model may be the main source of inhomogeneities. Rawinsonde data discontinuities, due to changes in instruments and observing practices, tend to have a timescale of approximately 10 years, although there are stations with much more frequent changes (Gaffen, 1994). It is thus important to detect the replacement date of the instrument model. For Argentina, approximate dates for rawinsonde replacement in the SMN Network are available from Duarte and Bischoff (1998) and are summarized in Table I. This Table includes not only the three stations analyzed in this research, but also includes a description for the complete network operated by the SMN. The reader interested in knowing the replacement dates of rawinsondes network all over the world can refer to Gaffen (1993). Detecting trends or inhomogeneities is not the scope of the present work, so Table I is shown solely for information purposes.

Velasco and Necco (1981) provide valuable information about the main characteristics of rawinsonde observations at rawinsonde stations in Argentina. Inspection of the mean monthly temperature profiles calculated for observations carried out from the late fifties into the early seventies shows that, on average, the temperature profile over CRD is quasi-isothermal above the tropopause both in winter and in summer. The change is smoother at EZE, and includes the presence of double tropopauses in January in the climatology, suggesting significant occurrence of *D-events* there. The beginning of the increase

Copyright © 2006 Royal Meteorological Society

DOI: 10.1002/joc

Table I. Approximate rawinsonde model replacement dates for the SMN network (from Duarte and Bischoff, 1998). In the period 1957–1964 stations 87750 (Bahía Blanca) and 87934 (Río Gallegos) used German–made Graw rawinsondes

Year	Rawinsonde model
1957	Väisälä RS11
1964	Väisälä RS13
1971	Väisälä RS15
1972	Väisälä RS18
1976	Väisälä RS21
1984	Väisälä, RS80 and RS15N

in stratospheric temperature with height can be clearly seen above the second tropopause. The temperature profile above the tropopause in July appears to be quasi-isothermal, same as over CRD. Profiles at RES do suggest an even more definite change in gradient sign above and below the tropopause, particularly in January. The July profile at RES also suggests the comparatively frequent occurrence of *D-events*, since a double tropopause is also present in the monthly mean climatology.

Figure 1(a) shows the quarterly mean tropopause height anomalies time series at each station. This time series has been built considering *ST* and *DF* together. Anomalies were calculated extracting the annual climatological wave (Jones, 1964) obtained by Fourier analysis. Once these anomalies were obtained, a seasonal average was calculated. With this procedure, the anomalies were destationalized, making different quarterly means comparable. A preliminary inspection does not show any visible trend in the tropopause height at all three stations and over the sampled period. However, it should be noted that when changes in rawinsonde models are taken into account, changes in the behavior of the anomalies could be observed (Gaffen *et al.*, 2000).

Between the years 1991 and 1995 there are two different behaviors for the seasonal anomalies at RES: the first two years have negative anomalies and the last two years have positive ones. It should be noted that although the anomalies do not exceed a unit of mean standard deviation at all stations, the anomaly range is smallest at CRD and largest over EZE, on average. Largest negative anomalies present at RES in mid 1987 need to be investigated in future works, because an El Niño event was present that year (Philander, 1990). Although there are large negative anomalies at EZE in mid 1987, they should not be taken into account because the number of samples available at that station considerably decreased during that period. Using the same criteria, it is difficult to deal with the negative anomalies detected at RES at the end of the period.

Figure 1(b) shows the number of samples per season. Except for specific years, each season is quite complete.

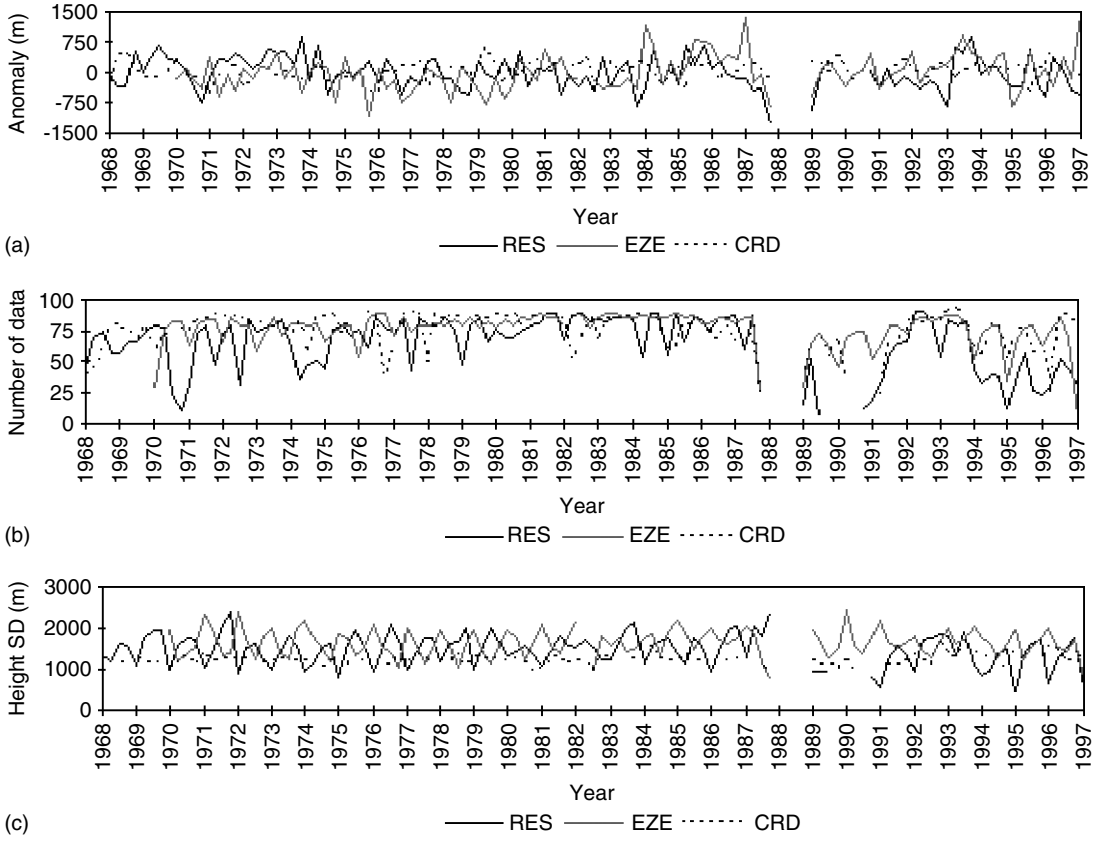

Figure 1. (a) Quarterly mean tropopause height anomalies time series. (b) Number of samples per season (c) Quarterly mean tropopause height anomalies standard deviation time series

Copyright © 2006 Royal Meteorological Society

DOI: 10.1002/joc

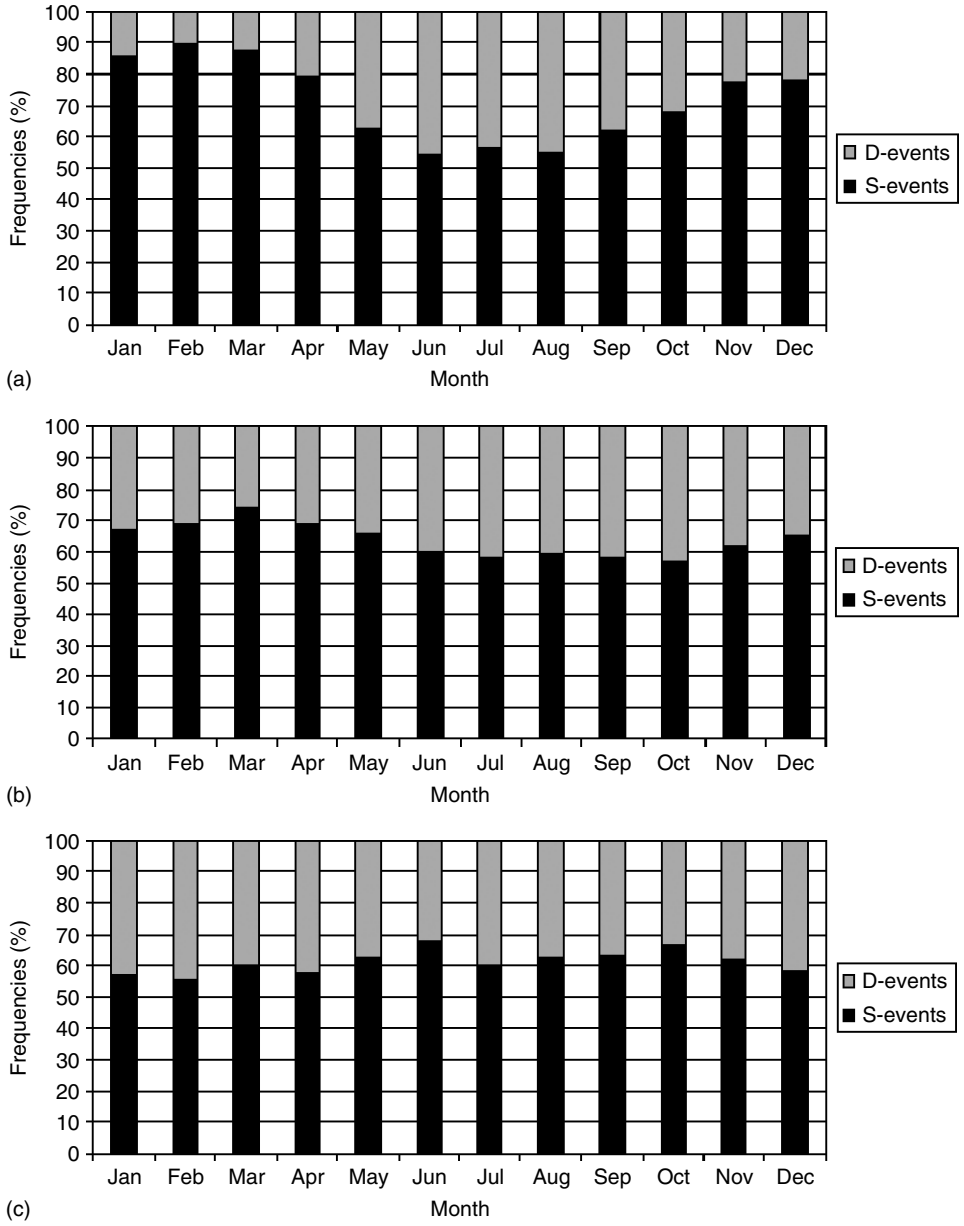

Figure 2. Mean monthly distribution of single and double tropopause events, as a monthly percentage of soundings available at: (a) RES, (b) EZE and (c) CRD

However, an important fall in data per season can be seen from mid 1987 till mid 1991 at all three stations, due to a severe national budget crisis during that period.

Figure 1(c) shows the quarterly mean tropopause height anomalies standard deviation time series at each station. An inspection of this figure shows that largest deviations occur over EZE and RES. Standard deviation of the mean quarterly anomalies also provides a preliminary view of the annual cycle of the tropopause variability. CRD shows a regular evolution from the very beginning of the data set till 1988. In addition, there seems to be no significant changes at this station after the break in the record. RES variability behaves in the opposite phase to EZE variability over all the period. However, a decrease in the RES variability can be seen after the break in the record. It is not yet clear whether this is due to the limited data available or the result of a real atmospheric process. This behavior is not seen at the other two stations.

RESULTS

S- and D-events statistics

The following analysis shows the relevance of considering the presence of not only *S-events* but also *D-events*. It is necessary to consider the relative rate of occurrence of *S*- and *D-events* at each of the stations.

Figure 2 shows the annual distribution of *S*- and *D-events* as a percentage of the monthly samples available. Significant differences in the frequency of annual cycles can be observed among the three locations. The lowest monthly percentage (12%) of *D-events* occurs at RES

Copyright © 2006 Royal Meteorological Society

DOI: 10.1002/joc

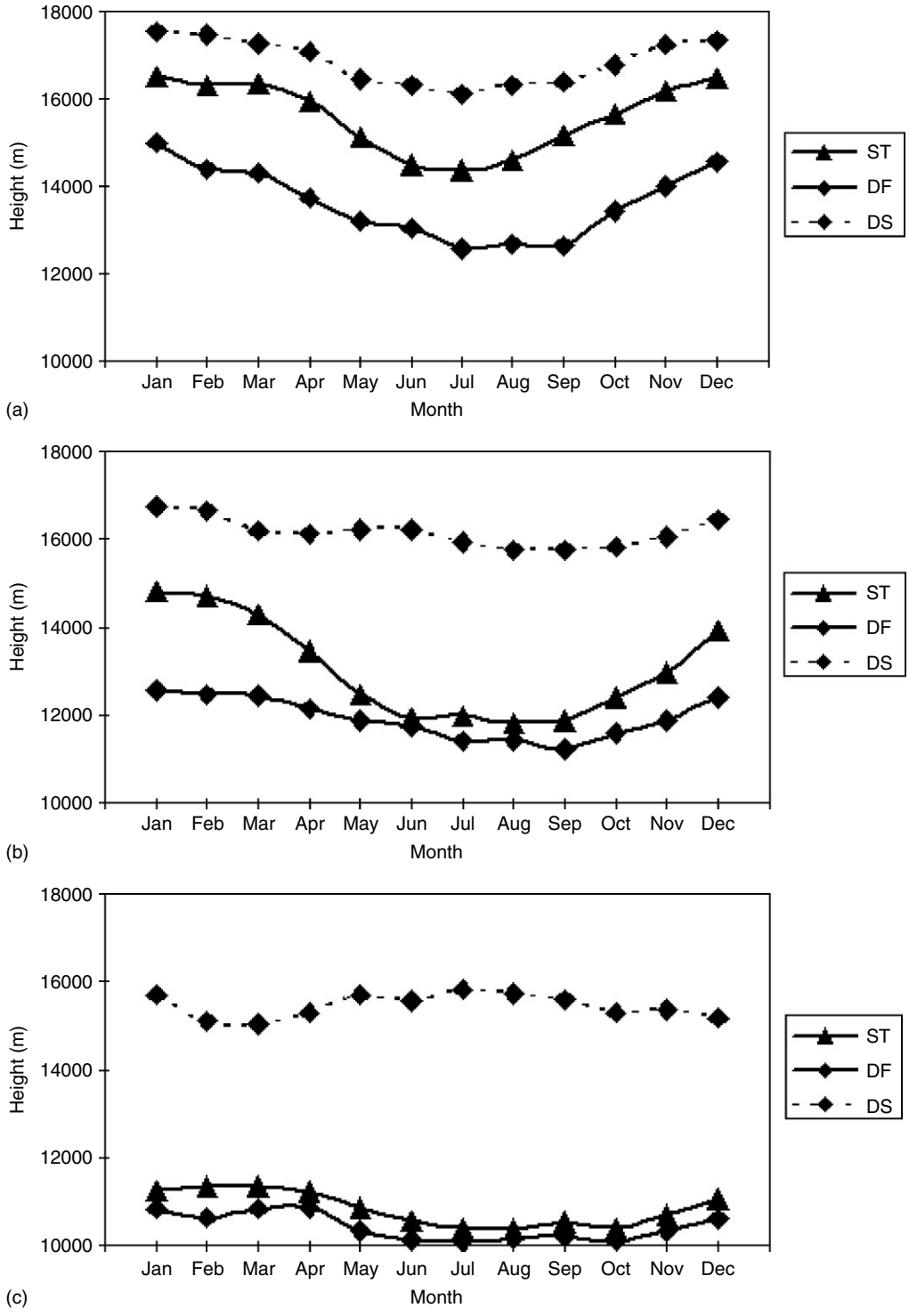

Figure 3. Monthly mean tropopause height at (a) RES, (b) EZE and (c) CRD

during the second part of summer, i.e. February and March. The most frequent (approximately 44%) *D-events* also occur at RES during winter. On the other hand, CRD has a reduced annual cycle with 45% occurrence of *D-events* in January and 30% in June. Thus, the annual cycle of *D-events* is reversed from the subtropics to mid-latitudes. EZE shows an intermediate behavior, with a minimum of *D-events* in March (25%) and their maximum occurrence ($\approx 42\%$) in late winter and early spring. The far greater range of annual frequency over RES could, nevertheless, be partly due to the non-detection of the *ST* or the *DS* during summer. Indeed, the average summer *DF* – close to 15 km as will be seen later – could lead to a second tropopause above the 100 hPa limit of the current data set. Broadly speaking, at any rate, the transition behavior over EZE confirms that the annual cycle behavior at RES is adequately described in the present analysis.

Copyright © 2006 Royal Meteorological Society

DOI: 10.1002/joc

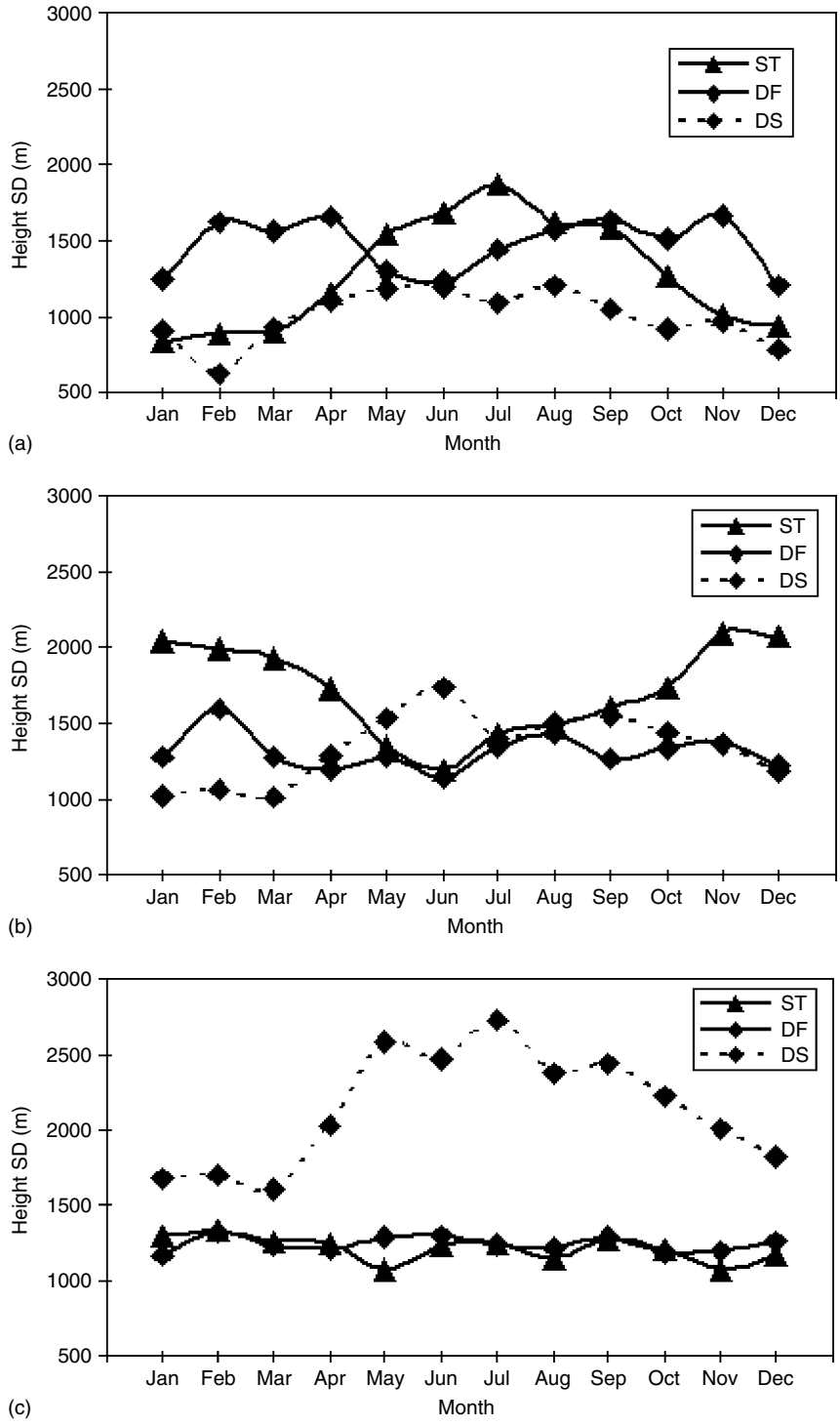

Figure 4. Monthly mean tropopause height standard deviation at: (a) RES, (b) EZE, and (c) CRD

Annual cycle

Height. Monthly mean height annual cycle can be observed in Figure 3. Mean tropopause height for *ST* oscillates around 11 km, with minima (maxima) in winter (summer). With regard to *D-events, DF* resembles the *ST* behavior and is found close to it, while *DS* is in opposite phase to both and located near 15-15.5 km.

ST annual cycle at EZE is distinct from that one at CRD, with a mean height near 13-13.5 km. The maximum is reached in January and minima are reached between June and September. The summer-to-winter mean height transition is fairly rapid while the winter-to-summer change is a somewhat slower process. When *D-events* are considered, *DF* shows approximately the same annual evolution with reduced amplitude. The heights of *DF* and *ST* are similar during the winter period. The behavior of the upper tropopause is the same as over CRD, with reduced annual amplitude as well.

Copyright © 2006 Royal Meteorological Society

DOI: 10.1002/joc

On the northern edge of the subtropics, over RES, *ST* annual cycle reaches maximum height between December and March and minimum in July. The mean height is 15.5–16 km. *DF* also has a well defined but asymmetric annual cycle, with minimum values between July and September and a fairly rapid rise in spring. At this station the annual cycle amplitude is fairly similar for the three kinds of tropopause events.

Note that the *DF* annual cycle over CRD is very similar to the *ST* annual cycle, while over EZE there are some larger differences between them during summer. Over RES, *DF* tends to be lower than *ST*, which seems to have an approximately mean position between the two *D-event* tropopauses. As a matter of fact, the relationship between *DF* and *ST* at EZE resembles that one of CRD in winter and RES in summer. Furthermore, while the separation between *DF* and *DS* varies during the year, on average it is of the order of 6 km over CRD, 5 km over EZE, and 4 km over RES, in other words, increasing southward. As expected, *S-events* show a decrease in height as latitude increases ($\approx$ 5 km between RES and CRD). The latitudinal change in height is in the order of 5 km for *DF* and in the order of 1–1.5 km for *DS*. All the characteristics mentioned above show a wide variety of ExTL behavior in this region.

The explained variance for each of the six computed harmonics, resulting from a harmonic least square fit applied to the tropopause height monthly mean, reveals that the first harmonic explains over 95% of the variance for *S-events* at all three sites, clearly showing the annual behavior. As to *D-events, DF* presents the same behavior as *ST*. The *DS* first harmonic decreases its explained variance in favor of the second one at EZE, and of the second, third, and sixth at CRD. Notwithstanding, RES presents no changes at all, the first harmonic still explaining more than 95% of the variance.

As already mentioned, the tropopause height standard deviation (σ_{H}) can provide insights into the variability of the samples. In particular, the monthly mean standard deviations are now considered for understanding the annual variability cycle in the tropopause height (Figure 4).

At CRD, σ_H^{ST} is between 1 and 1.3 km in the course of the year, with weak minima at the beginning of autumn and the end of spring, just when the Polar Jet stream begins its northward displacement (in the first case) and is returning (in the second case) (Palmén and Newton, 1971). σ_H^{DF} has a fairly stable behavior over the year, close to the σ_H^{ST} evolution, but σ_H^{DS} shows a well-defined annual cycle with a minimum value in summer and maximum values between April and October. For σ_H^{DS}, the growth is rather rapid in autumn but it tails off during spring. In this case, it oscillates between 1.7 and 2.7 km.

At EZE, σ_H^{ST} has a distinct annual cycle with largest values in summer ($\approx$2 km) and smallest in winter (1.3 km). A rapid drop can be observed in the autumn-to-winter change and a slower enhancement in the winter-to summer transition. Again, σ_H^{DF} has a weak annual cycle with a maximum in February. σ_H^{DS} has an annual evolution in opposite phase to the σ_H^{ST} one. As to *DS*, the variance is smaller in summer and early autumn, and maximum at the beginning of winter and spring. The first maximum, early in winter, could be due to the passage of both cold and warm fronts over the region at this time of the year. Interestingly enough, except for May, June and July, the values of σ_H^{ST} are larger than those for σ_H^{DS} and σ_H^{DF}.

The σ_H^{ST} annual evolution over RES shows an annual cycle with minima in summer (below 1 km) and maxima in winter (above 1.5 km), while σ_H^{DF} has a semiannual structure with maxima in autumn and spring. σ_H^{DS} does not have an important seasonal evolution, though the largest values occur during winter.

Thus, comparing the behavior in the three stations, EZE seems to present the most diverse σ_{H} annual evolution for all kinds of tropopause events. The highest variability occurs for *DS* in winter over CRD and for *ST* in summer over EZE.

Temperature. Figure 5 shows the annual cycle for the monthly mean temperature at all three sites. The temperature annual cycle over CRD has comparatively weak amplitude, in agreement with the height evolution and the vertical temperature profile described by Velasco and Necco (1981). Temperature maxima occur between November and February, while minima are reached between May and September. Temperature annual cycle for *ST* and *DF* are separated all year round by less than 5 °C, *S-events* being the cooler ones. *DS* temperature oscillates between *ST* and *DF*, and is closer to *ST (DF)* temperatures in summer (winter). This is in agreement with the temperature profiles at mid-latitudes, where there is very little temperature change with height in the vicinity of the tropopause.

The temperature annual cycle over EZE has a larger amplitude and is better defined than over CRD, which was also the case with tropopause height. For *ST*, a minimum temperature is reached during January–February and a maximum is reached in September. The spring-to-summer cooling occurs at a faster rate than the warming during autumn. The warmer *DF* temperature shows relative minima in June and during December – January, and two maxima (a secondary one in February and a broad one in late winter/early spring). *DS* has the same annual evolution as *ST*, albeit 3–5 °C cooler.

DF annual cycle at RES is fairly similar to the one for *ST* over EZE. The warmest period is during the late winter (July to September), and the cooler tropopauses are observed from December to January. At RES, *DS* temperatures are very close to the ones of *ST*s all year round, while *DF* is warmer by about 10 °C.

As can be seen from Figure 5, there is an inversion of phase for the annual cycle of any kind of tropopause in CRD with respect to the ones over RES. Besides, the *DF* annual cycle at EZE is indeed dominated by the annual wave, but with an important presence of the semi-annual wave too.

Copyright © 2006 Royal Meteorological Society

DOI: 10.1002/joc

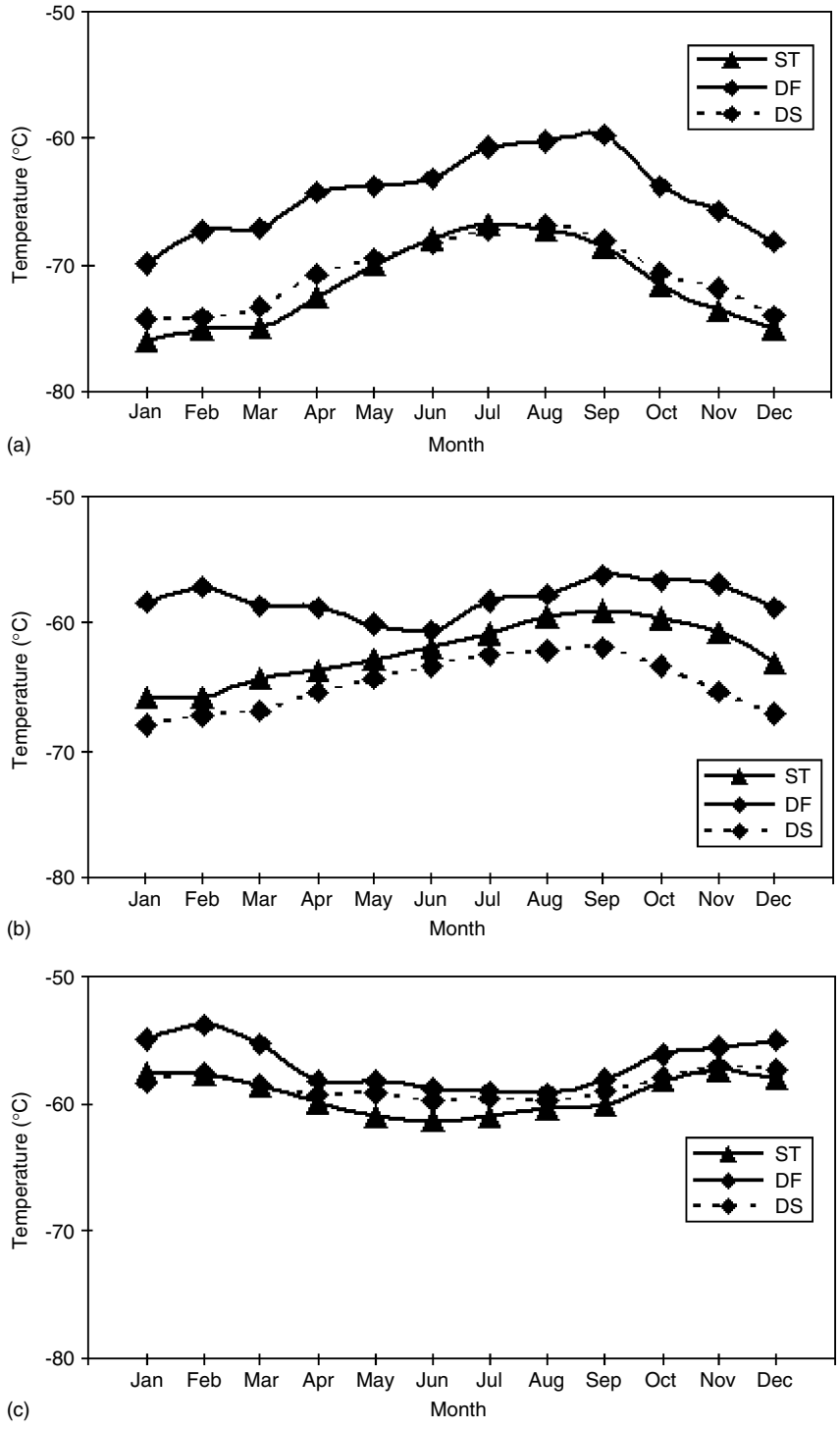

Figure 5. As in Fig. 3, but for tropopause temperature

The annual cycle of temperature is dominated by the first harmonic at all three stations and for any kind of tropopause in most cases. The only exception is *DF* at EZE. In that case, the annual and the semi-annual harmonics together explain about 90% of the variance.

Temperature standard deviation (σ_T) (Figure 6) shows different behaviors depending on the latitude and the kind of tropopause. σ_H^{ST} shows an oscillatory annual evolution at CRD, with a very weak range on the order of 1 °C, while at EZE the largest values are detected during the summer months, followed by an important drop in late summer/early autumn and a slow increase around August. At RES, the σ_T^{ST} annual cycle shows larger values during the autumn-to-spring period. σ_T^{DF} at CRD also shows a fairly stable behavior all year long, with a slight maximum in spring. With regard to EZE, σ_T^{DF} shows peak values in the middle of summer and winter. The variability of *DF* is further enhanced at RES, with largest values in February and March and an important

Copyright © 2006 Royal Meteorological Society

DOI: 10.1002/joc

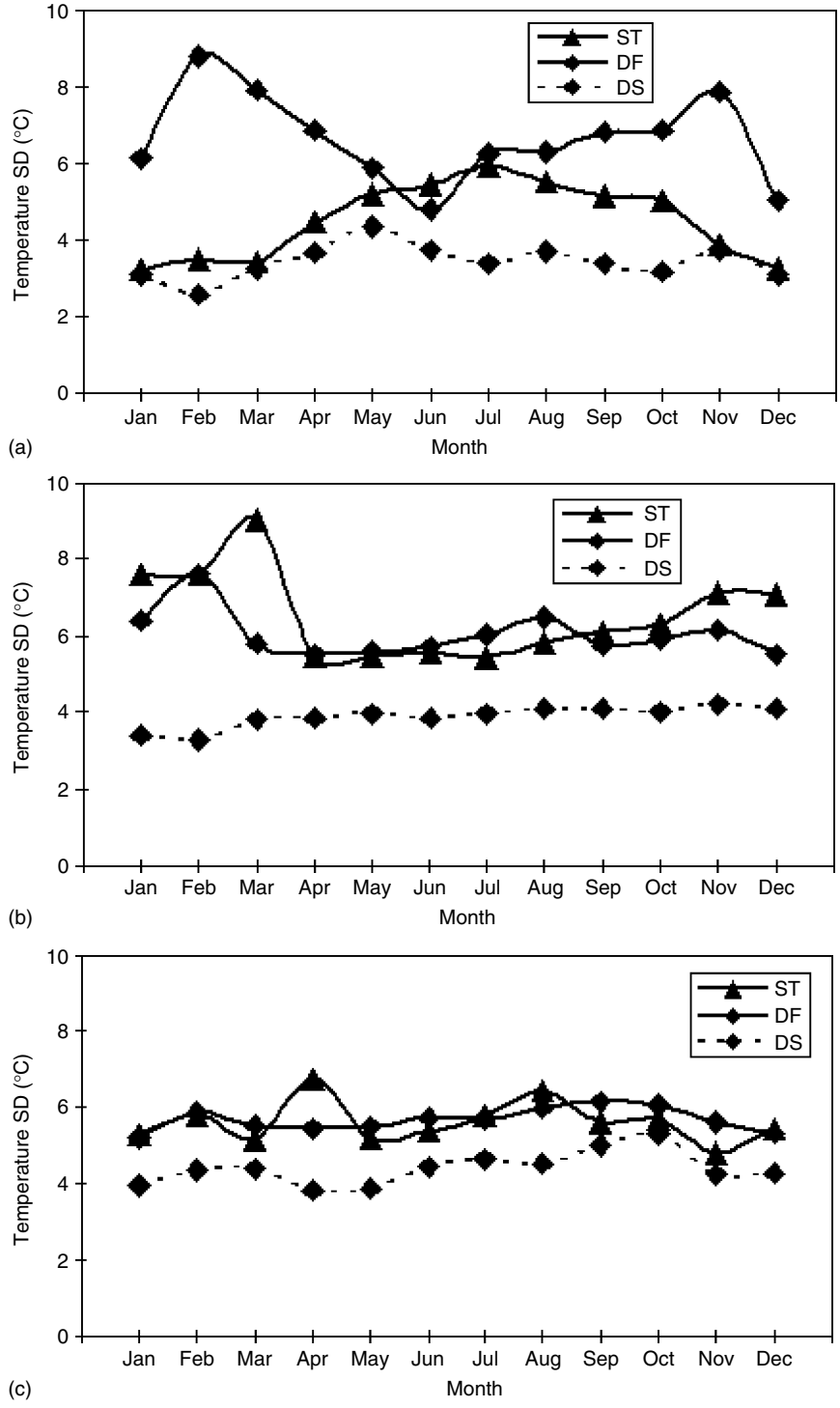

Figure 6. As in Fig. 4, but for tropopause temperature

secondary peak in late spring (November, ≈8 °C). On the other hand, σ_T^{DS} shows a very stable behavior at all three sites, with only minor fluctuations along the year. Such behavior is different from the σ_T^{ST} evolution at RES, which has a well-defined annual cycle.

A least square fit applied to the annual cycle of tropopause σ_T reveals that the annual wave dominance decreases with latitude for *S-events*. At CRD, all the harmonics seem to be important, with the exception of the fifth. With regard to *D-events*, the annual wave is dominant at CRD for σ_T^{DF}, and the semi-annual wave is dominant at the other two stations. Nevertheless, there is an important presence of the annual wave at RES and the semi-annual wave at CRD. Regarding σ_T^{ST}, half of the variance is explained by the annual wave at CRD, while the second and third harmonics are important as well; the annual wave by far dominates at EZE and is almost as important as the semi-annual one at RES. This can be related in a straightforward way to well-defined cycles in the tropopause temperature variability.

Copyright © 2006 Royal Meteorological Society

DOI: 10.1002/joc

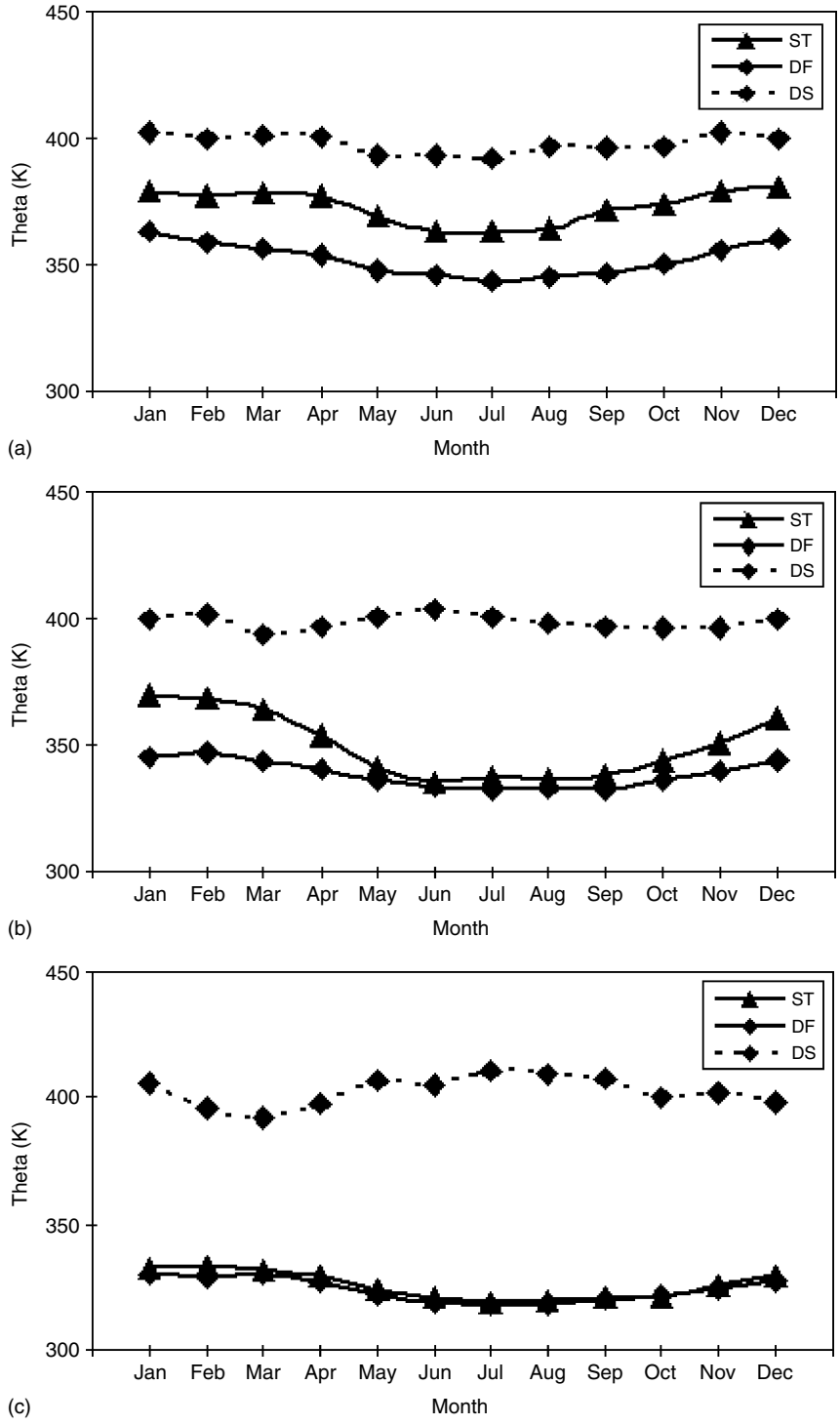

Figure 7. Same as in Fig. 3, but for potential temperature

Overall, the present analysis of the tropopause temperature behavior suggests that

- *ST* tropopause temperature annual cycle shows a decreasing amplitude with latitude, as well as a change in phase at higher latitudes, reaching minimum values during winter
- Temperature annual cycle over CRD for *S*- and *D-events* do not differ by more than 5 °C all year long and all of them are in phase
- Temperature annual cycle over RES is also in phase for *S*- and *D-events;* they do not differ by more than 8 °C all year long
- *DF* shows a prominent semi-annual cycle at EZE, and in general possesses the largest variability all year long at RES

Potential Temperature. Tropopause potential temperature (θ) climatological annual cycle is, in general, similar to height evolution, with maxima in summer and minima

Copyright © 2006 Royal Meteorological Society

DOI: 10.1002/joc

in winter. This result is not surprising. Figure 7 shows the annual cycle for every kind of tropopause discussed. As the plots show, the similarity holds for the evolution of *S*- as well as *D-event* situations. Nevertheless, an interesting feature is the value of θ^{DS}. Indeed, θ^{DS} surface oscillates in the vicinity of 380 to 400 K at all stations, while the values for θ^{ST} and θ^{DF} oscillate near 370, 350 and 340 K from north to south, as could be expected. θ^{DF} at RES is always lower than θ^{ST} by as much as 15 K. At EZE, the difference is larger during summer and there is no difference at all in winter. At CRD, both θ^{ST} and θ^{DF} have a very limited variability during the annual cycle.

Thus, the behavior of θ^{DS} poses an interesting challenge. Indeed, its value is remarkably close to that of the tropical cold-point tropopause (e.g. Gettelman and Forster, 2002) at all three stations.

Tropopause pressure frequency distribution

Hoinka (1998) studied the tropopause pressure distribution along 20 °E and 180 °E meridians, i.e. over landmasses and above the Pacific Ocean, respectively, using ECMWF reanalysis products and rawinsonde data. Given that ECMWF reanalysis calculations yield only one tropopause, *S-events* situations are considered first (Figure 8(a)). In this case the tropopause pressure distribution is approximately along 60 °W. The frequency distribution plot shows a large peak between 102 and 124 hPa over RES, with frequency of occurrence close to 40%. The frequency of occurrence shows a marked asymptotic tendency decreasing towards higher pressure values. At EZE, the magnitude of the peak frequency decreases and the distribution starts to flatten. At this station there are two maxima, the most important one being at 190–212 hPa, and the smaller one at 102–124 hPa. The distribution asymmetry observed over RES is also present over EZE. At mid-latitudes, over CRD, the pressure distribution becomes more symmetric, with a single maximum at the 212–234 hPa class interval.

In general these distributions are more peaked than those described in Hoinka (1998) along 20 °E. However, the present results are in good agreement with the ECMWF study, particularly over the South Pacific (180 °E). If *DF* is now included together with the *S-events* (Figure 8(b)), there will be some changes in the range and frequency distribution, although the overall aspects remain preserved. The frequency peak over RES will be reduced to a value of 30%. If *ST* and *DF* data are taken together, then the frequency distributions become closer to Hoinka's results, which is reasonable since the latter did not differentiate between these two states of the tropopause.

Statistics of tropopause extremes evolution

The above results need to be understood in terms of the tropopause dynamics and its coupling with troposphere and stratosphere dynamics. One way to obtain further insights on the underlying dynamic processes is to observe the temporal evolution of the extreme values. Very low or very high tropopause situations, and changes from one extreme to the other, are good parameters to study. Time sequences of persistence of the variable in the upper or lowermost quintiles of the height frequency distribution can be used for this purpose. Each quintile includes 20% of the data. Therefore, analyzing first and last quintiles will help us to understand the behavior of extreme events.

The persistence for *S-event* sequences as well as combined *S*- and *D-events* persistence sequences were considered. Tables II and III show the persistence frequency

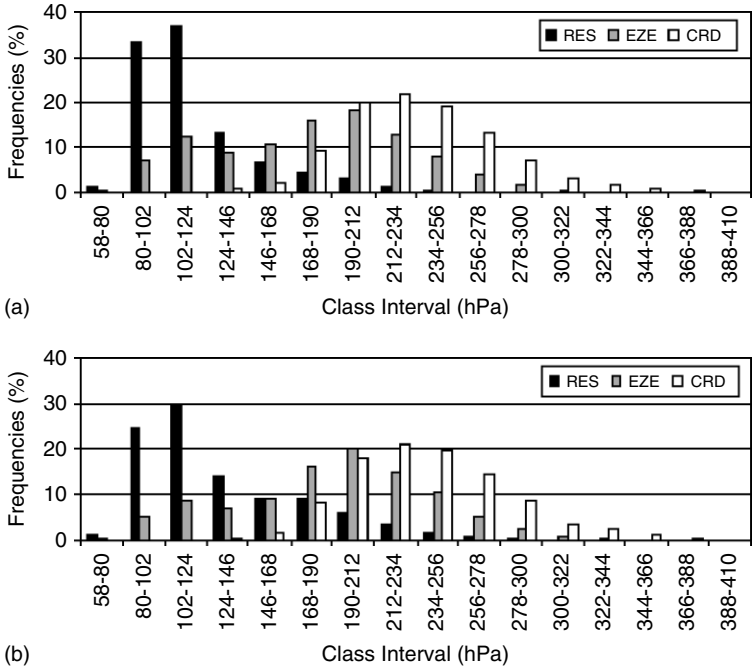

Figure 8. (a) Pressure frequency distribution for *ST*. (b) Pressure frequency distribution for combined *ST* and *DF*

Copyright © 2006 Royal Meteorological Society

DOI: 10.1002/joc

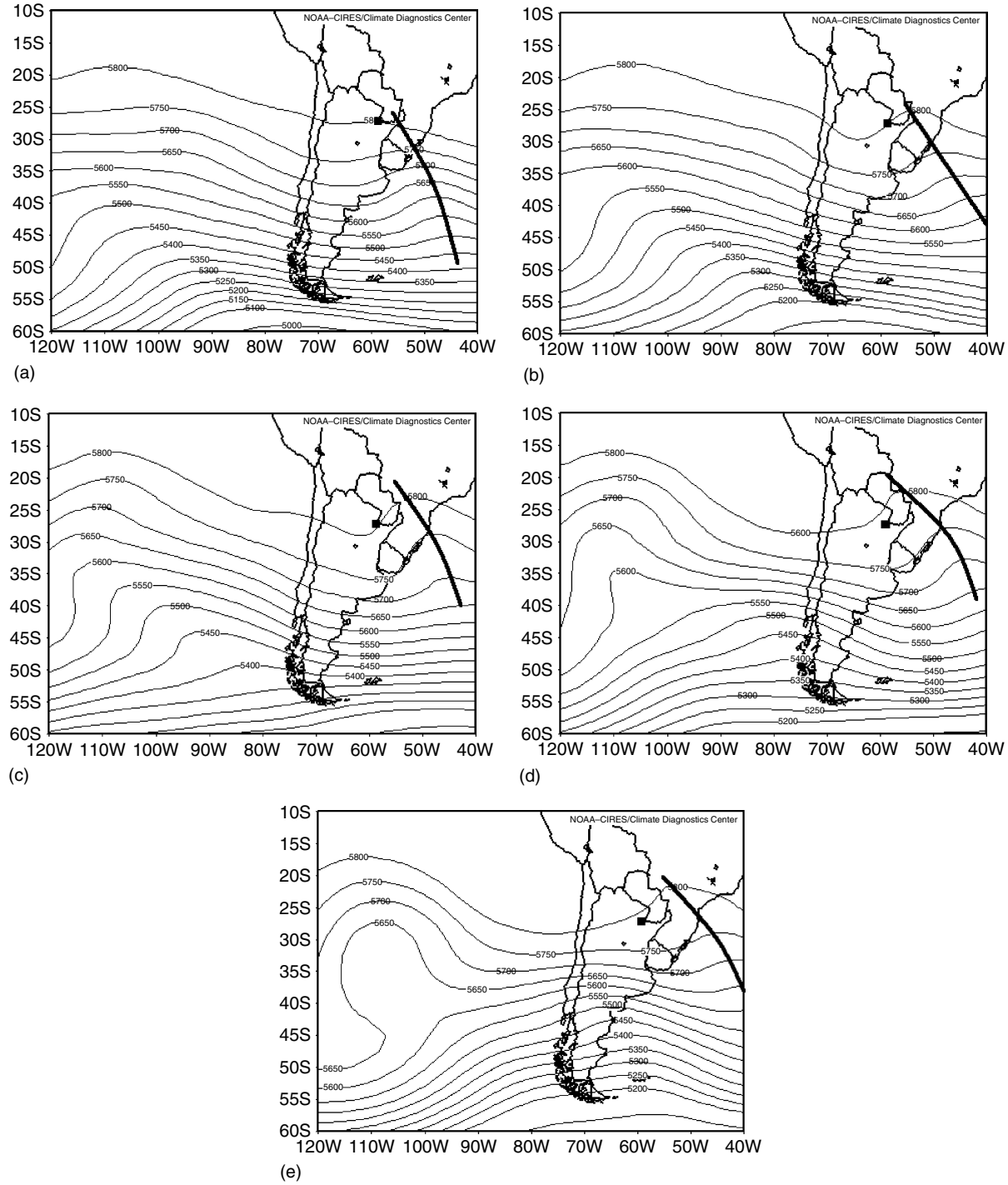

Figure 9. 500 hPa synoptic situations composite for the two 5–1111 cases registered at RES in winter (16 July 2003 and 6 August 1986). (a) corresponds to tropopause height within the limits of the last quintile and (b), (c), (d), (e) correspond to tropopause heights within the limits of the first quintile. The location of the station is marked with a bold square. Images provided by the NOAA-CIRES Climate Diagnostics Center, Boulder, Colorado, from their Web site at http://www.cdc.noaa.gov/

distribution for summer (DJF) as well as winter (JJA) months. Persistence is calculated by counting the number of consecutive days that the variable holds within the limits of the extreme quintiles. Each column of Tables II and III shows the number of consecutive days that the tropopause height holds within the limits of the corresponding quintile. During summer months, *S-event* sequences (II A) can most commonly remain in the first quintile (lowest tropopauses) for 2 days, there being little latitude differences. 3-day persistence sequences are about a third as frequent as the 2-day situations at RES and less than a fifth at CRD. Furthermore, for 3-day sequences there is a decrease in frequency as the latitude increases. 4- and 5-day sequences are rare but still occur over RES and EZE. Two 6-day sequences occurred only over EZE. If *ST* and *DF* are considered together, there are many more sequences (II B). Now, the 2-day sequences show a clear enhancement with latitude, i.e.

Copyright © 2006 Royal Meteorological Society

DOI: 10.1002/joc

such situations are almost twice as common at CRD than at RES. On the other hand, the 3-day persistence events are twice as frequent over EZE than at the other two sites. Furthermore, EZE shows the most varied and extended possibilities, including 5- 6- and 7-day sequences; an 8-day sequence did only occur over RES.

Last quintile (highest tropopauses) results (II C) during summer show significant 2-day persistence as well. It is interesting to note that the number of sequences is similar in both extreme quintiles. 3-day sequences for *S-events* also show a similar frequency and latitude behavior as the first quintile. The longer persistence sequences are even rarer at RES and CRD, while EZE exhibits some 6- and 7-day situations. When *DF* is included in the sequences (II D) the number of 2-day sequences is of the order of 50 events. 3-day sequences increase significantly at CRD, but not much at EZE and RES. On the other hand 4- and 5-day sequences increase at EZE.

Analysis of the sequences during winter months (Table III) yields somewhat different results. In *S-event* sequences (III A) there is an increase with latitude for 2-day first quintile sequences, a result that resembles the summer one. CRD shows almost twice as many such events as RES. 3-day sequences are now of the same order at all three stations, with occurrences between a fifth and a third of the number of 2-day situations. Some 4- and 5-day sequences occur at EZE and CRD and only one 6-day sequence at EZE. For 2-day sequences, the latitudinal change remains somewhat valid when *DF* is included (III B). While no changes are observed at RES for 3-day situations, there is an important increase over EZE and to a lesser extend over CRD. The largest changes appear when longer sequences are considered. 4-day sequences show a surprising increase at EZE and RES. Even if only a limited number of events are detected, these occur at all three sites for sequences longer than 4 days.

Results for the last quintile events are also interesting. *S-event* sequences (III C) show a weak increase with latitude for 2-day sequences. There are 4-day situations at EZE and CRD and 5-day situations only at EZE. When *DF* is included in the analysis (III D), there is an increase in the number of 2-day sequences without latitudinal differences. 3-day sequences become far more frequent at all three sites and 4-day situations also increase significantly with a fairly large number of events at EZE and CRD. Again, 5- or more day sequences appear, particularly at EZE and CRD.

Dealing with extreme events is more instructive if pictures of a suitable variable can be shown. Figure 9 shows a composite for the synoptic situation in 500 hPa when a jump from the last quintile (related to an *S-event*) to the first quintile (related to a *D-event*) occurs over

Table II. Persistence frequency of tropopause height in the first and last quintiles, in summer

SUMMER

(A) First Quintil *ST*

Station	2	3	4	5	6	7	8
RES	32	10	1	2	0	0	0
EZE	33	8	1	2	2	0	0
CRD	35	6	1	0	0	0	0

(B) First Quintil $ST + DF$

	2	3	4	5	6	7	8
RES	34	11	7	2	0	0	1
EZE	41	23	2	6	3	1	0
CRD	59	10	4	0	0	0	0

(C) Last Quintil *ST*

Station	2	3	4	5	6	7	8
RES	36	11	1	1	0	0	0
EZE	29	3	2	1	1	2	0
CRD	31	7	3	1	0	0	0

(D) Last Quintil $ST + DF$

	2	3	4	5	6	7	8
RES	48	16	1	1	0	0	0
EZE	49	5	4	4	1	1	1
CRD	50	30	3	2	0	0	0

Copyright © 2006 Royal Meteorological Society

DOI: 10.1002/joc

Table III. As in Table II, but for winter

WINTER

(A) First Quintil *ST*

Station	2	3	4	5	6	7	8
RES	24	9	0	0	0	0	0
EZE	35	6	1	2	1	0	0
CRD	40	8	4	1	0	0	0

(B) First Quintil $ST + DF$

	2	3	4	5	6	7	8
RES	44	9	12	3	2	1	0
EZE	61	23	9	1	1	0	1
CRD	58	18	6	3	1	1	0

(C) Last Quintil *ST*

Station	2	3	4	5	6	7	8
RES	32	8	0	0	0	0	0
EZE	39	8	2	2	0	0	0
CRD	42	12	3	0	0	0	0

(D) Last Quintil $ST + DF$

Station	2	3	4	5	6	7	8
RES	52	26	3	0	2	0	0
EZE	59	17	11	3	2	1	1
CRD	55	25	7	5	1	1	0

Table IV. Number of fifth-to-first quintile jump in tropopause height at the three stations

		Sequence					
Season	Station	5–1	5–11	5–111	5–1111	5–11111	5–111111
JJA	RES	20	6	–	2	–	1
–	EZE	10	1	–	–	–	–
–	CRD	10	–	–	–	–	–
DJF	RES	12	2	2	2	1	–
–	EZE	13	3	–	–	–	–
–	CRD	5	3	–	–	–	–

RES and the tropopause height 'persists' in that situation for four days. The source for this set of figures is the NCEP/NCAR Reanalysis (Kalnay *et al*., 1996). It starts when the tropopause height is located in the last quintile (Figure 9(a)). At any time between Figure 9(a)) and Figure 9(b) the fifth-to-first quintile jump occurs. In other words, there is a synoptic perturbation that leads to a single-to-double tropopause change. In Figure 9(b–e), the tropopause (DF) height is located in the first quintile. This sequence is named a 5–1111 sequence: the '5' means that the tropopause height over RES in the first map is within the limits of the fifth quintile; successive 1s after the hyphen denote the days in which the tropopause height 'persists' within the limits of the first quintile. This process is mainly linked to the passage of intense cold fronts, which results in the abrupt change of air masses (Coronel, 2001) and, consequently, in the tropopause height. The more the number of 1s that are located after the hyphen, the more intense the anticyclone following the cold front will be, because a more persistent situation is brought about. Figure 9 shows the development of an intense system over the Pacific Ocean and a quasi stationary trough in the northeastern part of Argentina. Attention must be focused on the second system though, which is marked by a bold line in each of the figure subparts. Following this example, Table IV shows the occurrence of these sequences for winter (JJA) and summer (DJF); the fifth-to-first quintile change takes

Copyright © 2006 Royal Meteorological Society

DOI: 10.1002/joc

place at any time between two consecutive days. These were selected after considering the change from one observation at the upper quintile to situations with one or more days 'persisting' in the first quintile. The largest number of sequences occurs over RES in winter, when cold fronts can reach lower latitudes, with 1- and 2-day persistence situations. Hoffmann (1971) studied different parameters related to the passage of fronts at Corrientes ($\varphi = 27.43\,^{\circ}$S, $\lambda = 58.75\,^{\circ}$O), a northern Argentine city separated from RES by only the wide Parana River. This city experiences the passage of 43.6 cold fronts per year, or 3.6 cold fronts per month. CRD and EZE show a similar number of 1-day situations solely in winter. Furthermore, only RES shows the occurrence of longer sequences both in winter and in summer. The change from a low tropopause into a very high one is the inverse option, but it is not very common and so will not be considered here.

DISCUSSION

The seasonal evolution of the occurrences of single and double tropopauses can be explained in terms of the main seasonal and synoptic scale processes in the region. During winter, the polar front moves north of CRD. It reaches its northernmost position near 30 °S, between July and September. This is the northernmost edge of the baroclinic zone, which peaks both near 60 °S and just south of the subtropical jet (Karoly *et al*., 1998, and references therein). In early spring it begins its southward retreat towards its southernmost summer position, near 50 °S, with reduced baroclinicity (Karoly *et al*., 1998). This annual evolution can help understand the frequency distribution of *S*- and *D-events*. As pointed out in Palmén and Newton (1971), breaks in tropopause and *D-events* can be associated with the passage of frontal systems. The contrast between the air masses at the edge of the frontal system can define the magnitude of the change in the tropopause height. Such a change can even lead to a separation into a lower and an upper tropopause. Coronel (2001) studied several properties of the air masses affecting Argentina, one of them being the equivalent potential temperature (θ_{ae}), which is perhaps the most conservative parameter used to characterize an air mass. At EZE and RES there is a difference of 20 K in the θ_{ae} values after the passage of a cold front. This difference is constant below 400 hPa over EZE, and below 800 hPa over RES.

Yet, Pan *et al*. (2004) considered the subtropical jet the primary source for *D-events*. The tropopause break in the vicinity of the subtropical jet is well documented. The following example shows that *D-events* can indeed occur in the presence of a frontal jet, in agreement with Palmén and Newton (1971). Figure 10 shows the state of the atmosphere when a double tropopause is detected in the vicinity of CRD in spring. The chosen sample corresponds to the passage of a cold front over CRD, and therefore a fifth-to-first quintile jump in the tropopause height occurs in the framework of a 5–11 sequence, as discussed in the previous section. The vertical cross section plots at 67 °W presented in Figure 10(a) and (b) show the evolution of the frontal jet, on 9 and 11 October 1992, in the vicinity of CRD. The corresponding temperature and dew-point soundings can be seen in Figure 10(c) and (d). In addition, Figure 10(e) sketches the regional map with the positions of the frontal jet over Central Patagonia and near CRD, and the subtropical jet in the region north of EZE and RES, over Northern Argentina and Southern Brazil, on these two days. On the 9th, when the frontal jet near 250 hPa is located south of CRD (Figure 10(a)), the rawinsonde profile shows a well-defined single tropopause (Figure 10(c)). On the 11th, the frontal jet, now at 300 hPa and slightly less intense, has moved north beyond CRD (Figure 10(b)). The temperature profile (Figure 10(d)) now shows a distinct double tropopause. The wind has a maximum intensity at the tropopause level, as can be seen from Figure 10(c–d). This frontal activity took place within the region of influence of the SH storm track, over southern South America at this time of the year (Karoly *et al*., 1998). This example thus verifies the conclusions reached by Palmén and Newton (1971) over southern mid-latitudes. The subsequent paragraphs show how significant this mechanism can be for the occurrence of *D-events*.

The frontal activity depicted is consistent with the location of NH deep Stratosphere-Troposhere Exchange (STE) events that, as shown in Stohl *et al*. (2003), coincides with the NH stormtrack during the winter months. In other words, the present analysis shows that jets in the vicinity of the tropopause – be it the subtropical jet or jets associated with frontal activity – can lead to tropopause breaks and double, or maybe even multiple, tropopause situations.

Cold fronts passages are the most common transient weather events over the continent. Mid-latitude cyclones coming from the Pacific cross the Andes and Argentina south of 35 °S, and take an east-southeasterly course into the Atlantic Ocean, while the cold front associated with the low-pressure center follows a north-eastward route. In general, the frontal penetrations are well spread over all seasons in all latitudinal bands. However, they are more frequent in the southern latitudinal belt (35 °S to 45 °S) and less frequent in the northern belt (north of 20 °S) (Oliveira, 1986).

Given that the horizontal temperature contrast between air masses is important to the impact of frontal systems in the tropopause, it is primarily in summer that the passage of cold fronts can produce tropopause breaks and *D-events* over CRD. Indeed, in winter the temperature contrast between the different air masses (i.e. between the local air mass and the air mass that follows the frontal zone and moves to the north) is comparatively small. During summer this contrast is larger owing to the large radiative warming of the local air masses over the continent. This larger change can lead to more pronounced effects upon the tropopause, including breaks in the tropopause and a resulting double tropopause. It

Copyright © 2006 Royal Meteorological Society

DOI: 10.1002/joc

is important to mention that during winter this region is under the influence of the subpolar low-pressure belt, which carries successive troughs associated to cold fronts, giving the dynamical conditions for the presence of double tropopause. Hence, the different mechanisms present in summer and winter lead to a more or less constant frequency of *D-events* over CRD.

On the other hand, more frequent *D-events* in winter and early spring over EZE are associated to the back and forth motion of the polar front and with the passage of cold fronts and their associated jet stream. Besides, the subtropical jet tends to place itself near the latitude of EZE in winter, and hence the associated baroclinic zone increases the chances of frontal perturbations in

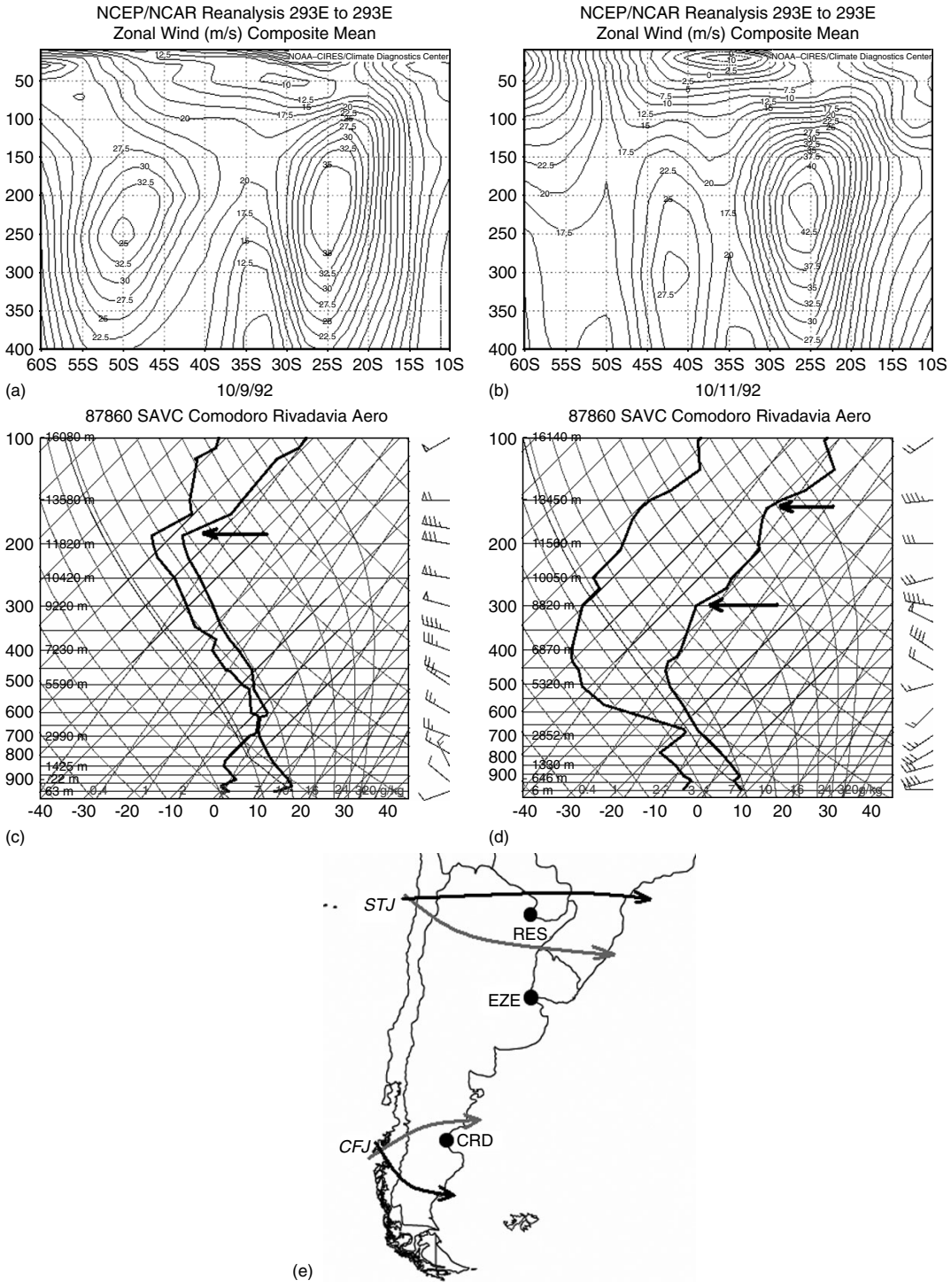

Figure 10. (a) Vertical cross section along 67 °W on 9 October 1992. (b) As in (a), but for 11 October 1992. (c) Temperature and dew-point soundings at CRD, 12UTC on 9 October 1992. The arrow marks the single tropopause position. (d) As in (c), but for 11 October 1992. Two arrows mark the two different observed tropopauses. (e) Position of the subtropical jet (STJ) and the jet associated to the cold front (CFJ) moving northward, on 9 October 1992 (black arrows), and 11 October 1992 (gray arrows). Circles indicate the location of the stations. Figures (a) and (b) provided by the NOAA-CIRES Climate Diagnostics Center, Boulder, Colorado, from their Web site at http://www.cdc.noaa.gov/

Copyright © 2006 Royal Meteorological Society

DOI: 10.1002/joc

the region. In summer, the much less chances of cold air surges in the region limit the probability of *D-events*. Nevertheless, it should be noted that the region is particularly influenced by the subtropical front in summer. This front is not so easily identified as the polar front, but it is also associated with tropopause breaks (Palmén and Newton, 1971).

Over RES, the behavior is similar to EZE but with a larger seasonal contrast. Even after taking into account the limitations of the data set, the large seasonal variability can be due to the passage of cold and warm fronts, but with a marked seasonal pattern. During summer, this region comes under the frequent influence of tropical air masses, with high temperatures and elevated water vapor content, which move from the Intertropical Convergence Zone into higher latitudes. In winter, the region is under the influence of colder systems, which have moved north, and occasionally comes under the effect of cold fronts traveling through Argentine Patagonia and central Argentina as far north as RES and even further, well into Brazil.

The tropopause height annual cycle, with minima in winter and maxima in summer, has a fairly similar range of approximately 2 km at all three sites. The annual cycle can explain more that 90% of the total variance for *S-events* at each of the stations and for *D-events* at RES. In other situations, higher harmonics need to be considered. Furthermore, the annual evolution of *DF* and *DS* shows a change in the thickness of the tropopause layer that they define on occurrence. This tropopause thickness varies from 6 km at CRD to 4 km at RES. As discussed above, *D-events* at all locations are primarily linked to the passage of cold fronts, particularly in winter. In summer, the tropopause behavior at RES and EZE could be influenced by the tropical tropopause, linked to the *DS*. It is interesting to note that during the May-1997 mini-hole event over central Argentina and Chile, trajectory calculations showed the possible advection of tropical air in the subtropical lower stratosphere, and the tropopause height at that time was close to that observed in the tropics, in the vicinity of 100 hPa (Canziani *et al*., 2002).

ST, DF and *DS* temperature at RES possess an annual cycle in agreement with those for the height annual cycle, i.e. opposite in phase, with maximum temperature found between May and September. At the other two stations the maximum *ST* temperature is detected towards spring and early summer at EZE, and summer at CRD. Furthermore, the layer determined by both *D-event* tropopauses at CRD has a distinct isothermal behavior practically all year round, just as it was pointed out by Velasco and Necco (1981) considering the errors in the tropopause temperature measurement. This feature is also true at EZE during the winter months, especially in June.

S-events tropopause height variability is maximum in winter (summer) at RES (EZE) and almost constant all year round at CRD. This feature differentiates *S-events* tropopause height behavior at a tropical station such as RES, from a transition station such as EZE, and a mid-latitude station such as CRD. Temperature variability of *S-events* maximizes at RES in winter, while at EZE it is fairly constant during that season and fairly stable all year round at CRD. In the first case, the sequence of cold and warm air masses with similar occurrence rates identify this subtropical region as a transition one in winter (Bischoff and Coronel, 1989). *ST* temperature and height variability at RES peaks around March and November, suggesting that there may be a significant alternation of subtropical and tropical air masses or even masses traveling so far north from southern mid-latitudes. Indeed, the very high tropopause in the summer months could imply a more stable presence of tropical air over the region. Furthermore, the relatively high variability between July and September could be due to cold air intrusions that can occur at this time of the year, occasionally even affecting southern Brazil as far as Rio de Janeiro (Satyamurty *et al*., 2002; Escobar and Bischoff, 2001; Garreaud, 2000). There are even cases in which the cold front crosses the Equator in the northern Amazon region, followed by a *friagem* (Fortune and Kousky, 1983). The term *friagem* refers to a period of cold weather in the middle and upper parts of the Amazon Valley and in eastern Bolivia.

Transition station EZE shows a maximum variability in summer both for the *ST* and *DF*. In summer, this region comes under the influence of warm and mildly cold air masses associated with a southward circulation driven by the South Atlantic anticyclone and northward flow perturbations that sometimes reach this latitude. In winter, warm air intrusions are far less frequent, owing to the northernmost displacement of the Polar Jet and the presence of more homogenous air masses.

As pointed out by Schwertfeger (1951), the summer-to-winter circulation change over southern South America is far shorter during the autumn (approximately two weeks) than the opposite transition during spring. From the above analysis we can consider that the largest variability can occur when this type of air masses change and such a situation can occur more frequently during the winter-to-summer transition, since it lasts much longer than the opposite transition. Such behavior is characteristic of the weather at EZE, from late August to October, and explains the shift in the occurrence of *D-events* towards the second half of the year. At RES, the more frequent air mass variability occurs in the winter months, and this is when we observe the more frequent *D-events*, with a tail toward the late spring months. On the other hand, air masses at CRD tend to be more stable, and the larger variability in air masses occurs in summer.

The calculation of the mean potential temperatures and their annual cycle provides an additional and interesting issue regarding the ExTL and its definition. Using observations obtained during airborne experiments carried out in 71 flights over northern extratropical latitudes, Pan *et al*. (2004) determined a region above the thermal tropopause in which the sampled air could have composition characteristics corresponding to mixed air masses

Copyright © 2006 Royal Meteorological Society

DOI: 10.1002/joc

of both tropospheric and stratospheric origin, i.e. a transition region between the troposphere and the stratosphere. They found that this transition layer was usually confined to the first 1–3 km above the thermal tropopause, but the thickness of the mixing layer above the tropopause could be as much as 4–6 km, particularly in the vicinity of the subtropical jet. Thus, Pan *et al*. (2004) suggest that this transition layer should be considered the extratropical tropopause layer or the ExTL. Our current observations yield height differences between the first and the second tropopause, ranging between 2 and 3 km at RES near the tropics and as much as 5–6 km at CRD at mid-latitudes, which is clearly consistent with the findings in Pan *et al*. (2004).

The present analysis, together with seminal concepts introduced in the 1990s, provides further insights for the ExTL definition. The fact that *DS* occurs at an almost constant potential temperature, virtually an isentropic surface, at least as far south as CRD, i.e. 45 °S, is very interesting. That such an isentropic surface coincides with the more commonly used definition of the tropical cold-point tropopause, when given in terms of θ, is highly suggestive. As defined in Gettelman and Forster (2002) the TTL layer is the layer between the minimum lapse rate and the cold-point tropopause. Pan *et al*. (2004) showed a typical example of the break in tropopause near the subtropical jet, in which the equatorward tropopause extends almost level from the tropics. The present results show that this upper tropopause can extend well into the mid-latitudes with practically no changes in height in terms of isentropic height, i.e. as a practically constant upper level for upper tropospheric jets – *both* the subtropical jet and jets associated with frontal activity.

It could be argued that the lower boundary of the tropopause layer in the extratropics would be given either in terms of *ST* or *DF* (which can be lower than *ST* at subtropical latitudes) and the upper boundary by the 380/400 K isentropic. Now, this region coincides with what Hoskins (1991) called the 'middle world' and Holton *et al*. (1995) called the lowermost stratosphere. These authors defined the 'middle world' or lowermost stratosphere as a region in which quasi horizontal mixing of tropospheric and stratospheric air can occur, with an upper limit in the vicinity of the 380 K isentrope. This region has isentropic surfaces that are shared with the troposphere at latitudes where comparatively more rapid STEs can occur, despite the dynamic tropopause transport barrier. Considering local/regional STE processes, such a definition agrees with observations in Pan *et al*. (2004), i.e. it is a region where significant mixing can occur. As noted in the previous paragraph, chemical composition in these regions has characteristics that result from the mixing of both down-welling stratospheric and tropospheric air, which episodically, but significantly, enters it quasi-isentropically in the subtropics and mid-latitudes through the tropopause (Stohl *et al*., 2003). There is no reason to believe that the processes involved in STE are significantly different between hemispheres. Nor is there any reason to doubt that the basic behavior of the double tropopause situations is any different in the NH from the results shown here. Indeed, the location of the deep STE events in the NH, as shown in Stohl *et al*. (2003), coincide with the NH stormtrack during the winter months, and significant exchanges also occur in the vicinity of the NH subtropical jet. As noted above, the sample event presented in Figure 10 is located in the vicinity of the SH storm track, and thus could lead to STE processes. In other words, the present analysis shows SH jets in the vicinity of the tropopause, be it the subtropical jet or jets associated with frontal activity, leading to breaks in the tropopause and double or maybe even multiple tropopause situations, in agreement with previous NH observations and STE results.

Considering the chemical composition results above the thermal tropopause in Pan *et al*. (2004), together with the rawinsonde observations in this analysis, which show (1) height ranges between the first and second tropopause in agreement with composition observations, and (2) that the *ST* has a virtually constant potential temperature in the range 380/400 K at least up to the mid-latitudes of the extratropics, and also considering that these two sets of observations are consistent with the dynamical/physical processes that are to be expected at those heights near the tropopause, it is then possible to define the ExTL as the region between the thermal tropopause and the 380 K isentropic. In other words, the ExTL is equivalent to Hoskins' 'middle world'or Holton's lowermost stratosphere.

CONCLUDING REMARKS

Understanding the occurrence and the characteristics of *D-events* is necessary to understand the mechanisms that drive STE and its seasonality. Relating such behavior with the synoptic variability of the ozone column at a given point is also important in order to be able to forecast surface UV-radiation levels. *D-events* in winter – mainly over CRD and to a lesser extent at EZE – could provide a fairly extended layer (5 to 6 km, on average) for exchange processes, given that these events are primarily linked to frontal systems or jets. The effects of the frontal jets as a transport barrier need to be further studied; there is evidence of enhanced STE processes as discussed, though. Thus, the determination of the full impacts of these broad ExTLs upon the exchange mechanisms requires a more detailed dynamic analysis, which is beyond the scope of the present work. Nevertheless, the present results, in particular, the rate of occurrence of such situations (35–40%), indeed show that there can be effective stratosphere–troposphere transfer processes during *D-events* and they could turn out to be important exchange mechanisms. Finally, the observed similarity of the *DS* potential temperature with the upper boundary of the TTL could provide further insights into the STE as well as on the dynamic coupling between the troposphere and the stratosphere.

Copyright © 2006 Royal Meteorological Society

DOI: 10.1002/joc

ACKNOWLEDGEMENTS

This study could have never been possible without the help of the Servicio Meteorológico Nacional. We are very grateful to them for providing the data used in this research. The authors also wish to thank the Inter American Institute for Climate Change Grant ISP-3-076, Agencia Nacional para la Promoción de la Ciencia y la Tecnología ANPCyT PICT-99 6588, Universidad de Buenos Aires X-095/2004-2006 grants and CONICET PIP 5276. We are indebted to the NCEP/NCAR for their websites online and for the availability of their reanalysis products. Valuable comments from two anonymous reviewers are also appreciated.

REFERENCES

Angell JK. 1991. Changes in tropospheric and stratospheric global temperatures, 1958–1988. *Greenhouse-Gas-Induced Climate Change: A Critical Appraisal of Simulations and Observations*, Schlesinger ME (ed). Elsevier: New York, NY; 231–247.

Appenzeller Ch, Holton JR, Rosenlof K. 1996. Seasonal variations of mass transport across the tropopause. *Journal of Geophysical Research* **101**: 15071–15078.

Bischoff S, Coronel A. 1989. Características estadísticas de las masas de aire en la troposfera de la región húmeda argentina. *Geoacta* **16**(2): 207–219.

Bjerknes J, Palmén E. 1937. Investigation of selected European cyclones by means of serial ascents, theorie der aussertropischen zyklonenbildung. *Meteorologische Zeitschrift* **54**(12): 462–466.

Bleck R, Mattocks C. 1984. A preliminary analysis of the role of potential vorticity in alpine lee cyclogenesis. *Contributions Atmospheric Physiology* **57**: 357–368.

Brasseur G. 1997. *The Stratosphere and Its Role in the Climate System*, *NATO ASI Ser.*, Vol. 54, Springer–Verlag: New York, NY.

Canziani PO, Compagnucci RH, Bischoff S, Legnani W. 2002. A study of impacts of tropospheric synoptic processes on the genesis and evolution of extreme total ozone anomalies over southern South America. *Journal of Geophysical Research* **107**(D24): 4741. doi:10.1029/2001JD000965.

Coronel AS. 2001. Climatología sinóptica de las masas de aire que afectan a la República Argentina, PhD in Meteorological Sciences Thesis, University of Buenos Aires, 83 pp.

Cox DI, Parker DE. 1992. The effects of changes in radiosonde equipment on upper-air "Climat" data. *Discussion Paper*, (E Division), Hadley Centre, Meteorological Office: Bracknell, England; 75.

Defant F, Taba H. 1957. The three fold structure of the atmosphere and the characteristics of the tropopause. *Tellus* **9**: 259–274.

Defant F, Taba H. 1958. The breakdown of the zonal circulation during the period January 8 to 13, 1956, the characteristics of temperature field and tropopause and its relation to the atmospheric field of motion. *Tellus* **10**: 430–450.

Duarte ML, Bischoff SA. 1998. *Informe interno del Departamento de Ciencias de las Atmósfera*.

Elliott WP, Gaffen DJ. 1991. On the utility of radiosonde humidity archives for climate studies. *Bulletin of the American Meteorological Society* **72**: 1507–1520.

Escobar GCJ, Bischoff SA. 2001. Criterio de detección de irrupciones de aire frío en la región central de argentina a partir de descensos interdiurnos de temperatura. *Meteorológica* **26**: 57–68.

Fortune M, Kousky VE. 1983. Two severe freezes in Brazil: precursors and synoptic evolution. *Monthly Weather Review* **111**: 181–196.

Gaffen DJ. 1993. Historical changes in radiosonde instruments and practices (WMO/TD-541). *Instruments and Observing Methods, Report 50*. World Meteorological Organization: Geneva, Switzerland; 123.

Gaffen DJ. 1994. Temporal inhomogeneities in radiosonde temperature records. *Journal of Geophysical Research* **99**(D2): 3667–3676.

Gaffen DJ, Santer B, Boyle J, Christy J, Graham N, Ross R. 2000. Multidecadal changes in the vertical temperature structure of the tropical troposphere. *Science* **28**: 1242–1245.

Garreaud R. 2000. Cold incursions over subtropical South America: mean structure and dynamics. *Monthly Weather Review* **128**: 2544–2559.

Gettelman A, Forster PMdeF. 2002. Definition and climatology of the tropical tropopause layer. *Journal of the Meteorological Society of Japan* **80**: 911–924.

Godske CL, Bergeron T, Bjerknes J, Bundgaard RC. 1957. *Dynamic Meteorology and Weather Forecasting*. Chapter 14, American Meteorological Society: Boston, MA.

Hoerling MP, Schaack TK, Lenzen AJ. 1991. Global objective tropopause analysis. *Monthly Weather Review* **126**: 3303–3325.

Hoffmann JA. 1971. Frentes, Masas de Aire y Precipitaciones en el Norte Argentino. *Meteorológica* **II**(1,2,3): 130–149.

Hoinka KP. 1997. The tropopause: Discovery, definition and demarcation. *Meteorologische Zeitschrift* **6**: 281–303.

Hoinka KP. 1998. Statistics of the global tropopause pressure. *Monthly Weather Review* **126**: 3303–3325.

Hoinka KP. 1999. Temperature, humidity and wind at the global tropopause. *Monthly Weather Review* **127**: 2248–2265.

Holton JR. 1990. On the global exchange of mass between the stratosphere and troposphere. *Journal of the Atmospheric Sciences* **47**: 392–395.

Holton JR, Haynes PH, McIntyre ME, Douglass AR, Rood RB, Pfister L. 1995. Stratosphere – troposphere exchange. *Reviews of geophysics* **33**(4): 403–439.

Hoskins BJ. 1991. Towards a PV-è view of the general circulation. *Tellus* **43AB**: 27–35.

Huovila S, Tuominen A. 1990. On the influence of radiosonde lag errors on upper-air climatological data in Finland 1951–1988. *Meteorological Publications N° 14*. Finnish Meterological Institute: Helsinki; 29.

Huschke RE (Ed.), 1959. *Glossary of Meteorology*. American Meteorological Society: Boston, Massachusetts, 638.

Jones RH. 1964. Spectral analysis and linear prediction of meteorological time series. *Journal of Applied Meteorology* **3**(1): 45–52.

Kalnay E, Kanamitsu M, Kistler R, Collins W, Deaven D, Gandin L, Iredell M, Saha S, White G, Woollen J, Zhu Y, Chelliah M, Ebisuzaki W, Higgins W, Janowiak J, Mo KC, Ropelewski C, Wang J, Leetmaa A, Reynolds R, Jenne R, Joseph D. 1996. The NCEP/NCER 40-Year Reanalyisis Project, *Bulletin of the American Meteorological Society* **77**(3): 437–471.

Karoly DJ, Dayton GV, Schrage M. 1998. General circulation. *Meteorological Monographs* **47**(49): 47–85.

Kochanski A. 1955. Cross sections of the mean zonal flow and temperature along 80 °W. *Journal of Meteorology* **12**: 95–106.

Kursinski ER, Hajj GA, Schofield JT, Linfield RP, Hardy KR. 1997. Observing Earth's atmosphere with radio occultation measurements using the global positioning system. *Journal of Geophysical Research* **102**(D19): 23429–23465.

Labitzke KG, van Loon H. 1999. *The Stratosphere, Phenomena, History and Relevance*. Springer–Verlag: Berlin 179 pp.

Lait LR. 1994. An alternative Form for Potential Vorticity. *Journal of the Atmospheric Sciences* **51**: 1754–1759.

Lakkis SG. 2005. Estudio de la tropopausa con observaciones a bordo de lo satélites SAC-C y CHAMP, M. Sc. in Physics Thesis, Universidad de Buenos Aires.

Luers JK, Eskridge RE. 1998. Use of Radiosonde Temperature Data in Climate Studies. *Journal of Climate* **11**(5): 1002–1019.

Morgan MC, Nielsen-Gammon JW. 1998. Using tropopause maps to diagnose mid latitude weather systems. *Monthly Weather Review* **126**: 2555–2579.

Nielsen-Gammon J. 2001. A visualization of the global dynamic tropopause. *Bulletin of the American Meteorological Society* **82**: 1151–1168.

Oliveira AS. 1986. *Interactions Between the South American Frontal Systems and the Amazonian Convection*, *INPE-4008-TDL/239* (Available from the library of the Instituto Nacional de Pesquisas Espaciais, Sao José dos Campos, SP, Brazil).

Palmén E, Newton CW. 1971. *Atmospheric Circulation Systems: Their structure and physical interpretation*. Academic Press: New York and London; 602.

Pan LL, Randel WJ, Gary BL, Mahoney MJ, Hintsa EJ. 2004. Definitions and sharpness of the extratropical tropopause: a trace gas perspective. *Journal of Geophysical Research* **109**: D23103. doi:10.1029/2004JD004982.

Philander SGH. 1990. *El Niño, La Niña and the Southern Oscillation*. Academic Press: San Diego, CA; 289.

Reed RJ. 1955. A study of a characteristic type of upper-level frontogenesis. *Journal of Meteorology* **12**: 226–237.

Copyright © 2006 Royal Meteorological Society

Reichler T, Dameris M, Sausen R. 2003. Determining the tropopause height from gridded data. *Geophysical Research Letters* **30**(20): 2042. doi:10.1029/2003GL018240.

Salby ML, Callaghan PF. 1993. Fluctuations of total Ozone and their relationship to Stratospheric Summer. *Bulletin of the American Meteorological Society* **65**: 1358–1365.

Satyamurty P, Ferreira Bustamante Fonseca S, Bottino MJ, Seluchi M, Maciel Lorenzo C, Gonzalvez de Gonzalvez L. 2002. An early freeze in southern Brazil in April 1999 and its NWP guidance. *Meteorological Applications* **9**: 113–128.

Schwertfeger W. 1951. Bases para el pronóstico a medio plazo de las condiciones de temperatura en el otoño en Buenos Aires. *Meteoros* **I**: 33–45.

Seidel DJ, Ross RJ, Angell JK, Reid GC. 2001. Climatological characteristics of the tropical tropopause as revealed by rawinsondes. *Journal of Geophysical Research* **106**: 7857–7878.

Shapiro MA. 1980. Turbulent mixing within tropopause folds as a mechanism for the exchange of chemical constituents between the stratosphere and the troposphere. *Journal of the Atmospheric Sciences* **37**: 994–1004.

Shepherd TG. 2002. Issues in Stratosphere-troposphere coupling. *Journal of the Meteorological Society of Japan* **80**: 769–792.

Smith WL, Woolf HM, Hayden CM, Wark DQ, McMillin LM. 1979. The TIROS-N operational vertical sounder. *Bulletin of the American Meteorological Society* **60**: 1177–1187.

Spencer RW, Christy JR, Grody NC. 1990. Global atmospheric temperature monitoring with satellite microwave measurements: method and results: 1979-84. *Journal of Climate* **3**: 1111–1128.

Steinbrecht W, Claude H, Köhler U, Hoinka KP. 1998. Correlations between tropopause height and total ozone: implications for long term changes. *Journal of Geophysical Research* **103**: 19183–19192.

Stohl A, Bonasoni P, Cristofanelli P, Collins W, Feichter J, Frank A, Forster C, Gerasopoulos E, Gäggeler H, James P, Kentarchos T, Kromp-Kolb H, Krüger B, Land C, Meloen J, Papayannis A, Priller A, Seibert P, Sprenger M, Roelofs GJ, Scheel HE, Schnabel C, Siegmund P, Tobler L, Trickl T, Wernli H, Wirth V, Zanis P, Zerefos C. 2003. Stratosphere-troposphere exchange: A review, and what we have learned from STACCATO. *Journal of Geophysical Research* **108**(D12): 8516, doi:10.1029/2002JD002490.

Suzuki S, Asahi M. 1978. Influence of solar radiation on the temperature measurement before and after the change of the length of suspension used for the Japanese radiosonde observation. *Journal of the Meteorological Society of Japan* **56**: 61–64.

Thuburn J, Craig GC. 1997. GCM tests of theories for the height of the tropopause. *Journal of the Atmospheric Sciences* **54**: 869–882.

Van Haver P, De Muer D, Beekmann M, Mancier C. 1996. Climatology of tropopause folds at midlatitudes. *Geophysical research letters* **23**(9): 1033–1036.

Velasco I, Necco GV. 1981. Características del campo térmico de la atmósfera libre de la República Argentina. *Meteorológica* **XII**(2): 7–22.

Willett HC. 1944. *Descriptive Meteorology*. Academic Press: New York, NY; 310.

Wirth V. 1995. Diabatic heating in an axisymmetric cut-off cyclone and related stratosphere – troposphere exchange. *Quarterly Journal of the Royal Meteorological Society* **121**: 127–147.

World Meteorological Organization (WMO). 1957. Definition of the tropopause. *World Meteorological Organization Bulletin* **6**: 136 pp.

World Meteorological Organization (WMO). 1978. The compatibility of upper-air data: Part I, Research on compatibility of data from radiosondes, rocketsondes and satellites, by F. G. Finger and R. M. McInturff; Part II, The compatibility and performance of radiosonde measurements of geopotential height in the lower stratosphere for 1975-76, by E. A. Spackman, *WMO 512, Tech. Note 163*, 103 pp.

World Meteorological Organization (WMO). 1992. *International Meteorological Vocabulary WMO/OMM/BMO – No. 182*. (Second edn). Secretariat of the World Meteorological Organization–Geneva–Switzerland: Geneva; 784.

World Meteorological Organization (WMO). 2003. Global Ozone Research and Monitoring Project. Report N° 47. Geneva: Switzerland.

Yuchechen AE, Lakkis SG, Canziani PO. 2005. Estudio de las observaciones de tropopausa sobre el Cono Sur de Sudamérica mediante GPS a bordo de los satélites SAC-C y CHAMP. *Meteorológica*. In press.

Zängl G, Hoinka KP. 2001. The tropopause in the polar regions. *Journal of Climate* **14**: 3117–3139.

Copyright © 2006 Royal Meteorological Society